PHYSICAL REVIEW B VOLUME 46, NUMBER 9 1 SEPTEMBER 1992-I

Dipole approximation in electron-energy-loss spectroscopy: L-shell excitations

D. K. Saldin and Y. Ueda
Department of Physics and Laboratory for Surface Studies, University of Wisconsin–Milwaukee, P.O. Box 413, Milwaukee, Wisconsin 53201
(Received 20 April 1992)

Using analytic expressions for core and excited-state electron wave functions, we examine the validity of the "dipole approximation" in electron-energy-loss spectroscopy (EELS) due to the L-shell excitations of atoms up to an atomic number of about 50. We derive analytic expressions for the limiting magnitude q_d of the momentum transfer vector and compare them with expressions for the most likely value of q for a range of chemical elements. We conclude that, although the dipole approximation is good for all L edges for the high incident primary energies typical of transmission EELS, it is of doubtful validity for the $L_{II\text{-}III}$ edges of the heavier elements for the relatively low primary energies used to increase surface sensitivity in reflection EELS.

I. INTRODUCTION

Studies of the fine structure close to absorption edges on x-ray-absorption spectra (XAS) due to the excitation of atomic core electrons have enabled much information to be deduced about both the electronic and atomic structure around specific chemical species in materials. The region within a few tens of electron volts from an absorption edge, which is known as the x-ray-absorption near-edge structure (XANES),[1] may be regarded as a probe of the unoccupied local density of states at the absorbing atom. The part of the spectrum further away from the edge is known as the extended x-ray-absorption fine structure (EXAFS),[2–5] from which atomic structural information may be extracted by Fourier transform techniques. In view of the fact that x-ray-absorption experiments usually have to be performed at remote synchrotron radiation facilities, much attention has been paid recently to the possibility of extracting similar information from electron-energy-loss spectra (EELS),[6–10] which exhibit similar absorption edge structure. The parts of the spectra analogous to XANES are known as the electron-energy-loss near-edge structure (ELNES),[11] and those parts more distant from the absorption edges, corresponding to EXAFS, are known as the extended electron-energy-loss fine structure (EXELFS).[12]

In the limit of small momentum transfer in an electron-energy-loss process, the matrix element for the inelastic scattering event reduces to one of essentially the same form as that for x-ray absorption, namely, an electric-dipole (or "optical") matrix element. Matrix elements of this reduced form are said to employ the "dipole approximation."[6] In this limit, electric-dipole selection rules relate the angular-momentum quantum numbers of the core and ejected electrons. Under such circumstances, an electron-energy-loss spectrum bears a remarkable similarity to the corresponding x-ray-absorption spectrum, and can be successfully interpreted in terms of the relatively well-developed tools of x-ray-absorption theory. However, the observation of so-called "nondipole" effect[13–16] makes clear that the x-ray-absorption model cannot be used indiscriminately for the interpretation of EELS spectra. Under such circumstances, analysis of EELS spectra requires a more complicated theory.[15–22] Clearly, efficient interpretation of EELS would benefit considerably from a precise knowledge of the limits of validity of the dipole approximation.

There has been some theoretical work in the past to compare the "dipole" and "nondipole" contributions to an EELS signal by numerical computation of the relevant matrix elements.[15,16,22,23] However, due to the significant numerical labor involved, these have been restricted to a few selected chemical elements, and for restricted ranges of the energy of the incident primary electron and that of the ejected core electron. In our recent paper,[24] we have attacked this problem in a more systematic way, using analytic representations of the core electrons before and after their excitations by the incident primary electron beam. In the quoted paper,[24] we investigated the limits of the dipole approximation for K-shell excitations of elements of atomic number up to about 50 (the upper limit of a nonrelativistic theory). The aim of this paper is to extend our study to L-shell excitations of about the same range of elements.

II. THE X-RAY-ABSORPTION COEFFICIENT AND THE EELS SCATTERING CROSS SECTION

A deeply bound atomic core electron experiences strong coupling between its own orbital and spin angular momenta. Consequently, its orbital angular momentum quantum numbers, $L=(l,m)$ and corresponding spin quantities $(\frac{1}{2},s)$ cease to be good quantum numbers. Instead the state is characterized by those of total angular momentum (j,m_j). This is of particular relevance when considering the excitation of all inner shells except the K shells (for which $l=0$), since the spin-orbit coupling lifts the degeneracy of states with the same l but different j. In the case of L-shell excitation, which is the focus of this

paper, the possible core states belong to the $L_{\rm I}$ ($l=0$, $j=\frac{1}{2}$), $L_{\rm II}$ ($l=1$, $j=\frac{1}{2}$), and $L_{\rm III}$ ($l=1$, $j=\frac{3}{2}$) subshells, in order of increasing energy, according to the usual notation in x-ray spectroscopy. If a core electron is given sufficient energy by an absorbed x-ray photon to eject it from the atom, the spin-orbit coupling is so reduced that the orbital, $L'=(l',m')$ and spin quantum numbers $(\frac{1}{2},s')$ may be regarded as good quantum numbers of the excited state. For L-shell excitations, therefore, we must consider electronic transitions from the core state:

$$\phi_{nlj}(r)Y_{jm_j}(\hat{\mathbf{r}}) , \tag{1}$$

to the excited state,

$$R_{l'}(\epsilon,r)Y_{l'm'}(\hat{\mathbf{r}})\sigma_{1/2,s'} . \tag{2}$$

In the expressions above, ϕ represents the radial wave function of the core state, R that of the excited state of energy ϵ, Y a spherical harmonic, n the principal quantum number of the core state, $\mathbf{r}$ a position coordinate, and σ a spin state. In the following we will make the usual approximation that

$$\phi_{nlj}(r)\simeq\phi_{nl}(r) , \tag{3}$$

i.e., that, to first order, the spin-orbit interaction does not perturb the core wave functions.

In x-ray absorption the transition between these two states is induced by the perturbation:

$$i\omega\,\mathbf{A}\cdot\mathbf{r} , \tag{4}$$

where $\mathbf{A}$ is the magnetic vector potential of the x rays. The transition rate for unpolarized x rays or a polycrystalline sample (i.e., averaging over all directions of $\mathbf{A}$) can be calculated on first-order perturbation theory to be[1,25]

$$W^{nlj}=-\frac{8\pi}{3}\kappa\omega^2A^2(2j+1)\sum_{L'}[M_{nl,\epsilon l'}]^2\frac{\mathrm{Im}(\tau_{L'L'})}{\sin^2\delta_{l'}}\left[\begin{pmatrix} l' & 1 & l \\ 0 & 0 & 0\end{pmatrix}\right]^2 , \tag{5}$$

where κ is the wave vector of the ejected core electron, ω is the angular frequency of the incident x rays,

$$M_{nl,\epsilon l'}=\int_0^\infty\phi_{nl}(r)(Ar)R_{l'}(\epsilon,r)r^2dr , \tag{6}$$

and

$$\begin{pmatrix} l' & 1 & l \\ 0 & 0 & 0\end{pmatrix} \tag{7}$$

is a Wigner $3j$ symbol.[26]

In (5), τ is the site-diagonal scattering path operator[27] of the exciting atom in its host environment in a solid. Writing it as a matrix in the angular momentum representation,

$$\tau=it(1-\mathbf{St})^{-1} , \tag{8}$$

where

$$t_{l'l''}=i\sin\delta_{l'}e^{i\delta_{l'}}\delta_{L'L''} \tag{9}$$

is the atomic t matrix, $\delta_{l'}$ being the phase shift of angular momentum l'. The quantity $\mathbf{S}$ in (8) is the backscattering matrix of the atoms surrounding the absorber, and is responsible for the fine structure on x-ray-absorption spectra. It may be evaluated by a multiple scattering cluster calculation.[1,28]

The quantity corresponding to (5) in EELS is the differential scattering cross section per unit solid angle Ω and per unit energy range E_f of an electron of primary energy E_i, suffering an energy loss to a final energy E_f, namely[18,19,25]

$$\frac{\partial^2\sigma^{nlj}}{\partial E_f\partial\Omega}=-\frac{1}{\pi^2}\frac{k_f}{k_i}\kappa\frac{1}{q^4}(2j+1)\sum_{L'l''}(2l''+1)\times[F^{l''}_{nl,\epsilon l'}(q)]^2\frac{\mathrm{Im}(\tau_{L'L'})}{\sin^2\delta_{l'}}\left[\begin{pmatrix} l' & l'' & l \\ 0 & 0 & 0\end{pmatrix}\right]^2 , \tag{10}$$

where k_i and k_f are the wave vectors of the primary electron before and after energy loss, q is the magnitude of the momentum transfer vector

$$\mathbf{q}=\mathbf{k}_i-\mathbf{k}_f \tag{11}$$

and we have averaged over all directions of this vector:

$$F^{l''}_{nl,\epsilon l'}(q)=\int_0^\infty\phi_{nl}(r)j_{l''}(qr)R_{l'}(\epsilon,r)r^2dr \tag{12}$$

is a radial matrix element for the atomic transition and $j_{l''}$ a spherical Bessel function of order l''. In the derivation of (10) we have neglected effects due to the exchange of the incident and core electrons, since they are believed to have little effect of the EELS cross section.[21]

Except perhaps very close to an absorption edge, backscattering of the ejected core electrons is small, i.e., $\mathbf{S}$ is small, and we may take

$$\tau\simeq it . \tag{13}$$

Then (5) and (10) reduce to

$$W^{nlj}=\frac{8\pi}{3}\kappa\omega^2A^2(2j+1)\sum_{l'}(2l'+1)[M_{nl,\epsilon l'}]^2\times\left[\begin{pmatrix} l' & 1 & l \\ 0 & 0 & 0\end{pmatrix}\right]^2 \tag{14}$$

and

$$\frac{\partial^2\sigma^{nlj}}{\partial E_f\partial\Omega}=\frac{1}{\pi^2}\frac{k_f}{k_i}\kappa\frac{1}{q^4}(2j+1)\sum_{l'}(2l'+1)\sum_{l''}(2l''+1)\times[F^{l''}_{nl,\epsilon l'}(q)]^2\left[\begin{pmatrix} l' & l' & l \\ 0 & 0 & 0\end{pmatrix}\right]^2 , \tag{15}$$

respectively. Alternatively, (14) and (15) may be regarded as the x-ray-absorption rate and the EELS scattering

cross section for an atom in free space.

In order to see the relation between (14) and (15) note that the Bessel functions in (12) may be expanded in series of ascending powers of q:

$$j_0(qr)=1-\frac{(qr)^2}{6}+O[(qr)^4]\ , \tag{16}$$

$$j_1(qr)=\frac{(qr)}{3}-\frac{(qr)^3}{30}+O[(qr)^5]\ , \tag{17}$$

$$j_2(qr)=\frac{(qr)^2}{15}+O[(qr)^4]\ , \tag{18}$$

$$j_3(qr)=O[(qr)^3]\ , \tag{19}$$

$$\vdots\ .$$

Substituting (16)–(19) into (15) we see that the EELS differential cross section may be written as a power series in q. The lowest power of q in Eqs. (16)–(19) is q^0 in (16), but this term does not contribute to (15) due to the orthogonality of the core and excited-state wave functions in (12). The next lowest power of q is q^1 in (17). For sufficiently low values of q therefore, the dominant term in the sum over l'' in (15) will be that with $l''=1$, and keeping only the term linear in q in the series expansion of $F^1_{nl,\epsilon l'}(q)$, we see that (15) reduces exactly to the form (14) except for the factors outside the summation over l'. Hence, it follows that the expression (15) for the EELS cross section becomes essentially identical to that for the x-ray-absorption rate (14) provided the magnitude q of the momentum transfer vector (11) is sufficiently small. In this paper we will make quantitative estimates of what is meant by *sufficiently small* in the case of L-shell excitations of chemical elements with atomic numbers up to about 50.

In fact, (10) will reduce to essentially (5) in the same limit, but since we are searching for general conditions and are not too concerned with the structure-dependent small quantities **S**, we will concentrate on the relationship between the simpler expressions (15) and (5) in the rest of this paper.

Just as the linear dependence of $M_{nl,\epsilon l'}$ on A in (6) results in the x-ray-absorption rate W proportional to A^2, the term linear in q in $F^1_{nl,\epsilon l'}$ gives rise to a term in the EELS scattering cross section proportional to q^2. Since x-ray absorption in atoms is caused by induced electric-dipole moments, the term proportional to q^2 is known as the dipole contribution to the EELS cross section. Our strategy will be to compare the magnitude of the terms proportional to q^2 (the lowest power of q) with that of the next-highest power, namely q^4. As we see below, this leads naturally to a criterion for an upper limit q_d of the magnitude of the momentum transfer vector (11) beyond which the dipole terms will not dominate the EELS scattering cross section (26).

III. THE LIMITING MAGNITUDE q_d OF THE MOMENTUM TRANSFER VECTOR

A. $L_{\rm I}$ edge

$L_{\rm I}$ edges in XAS or EELS are due to the excitations of $2s$ electrons. As in the case of the K edges (which are due to $1s$ excitations, the subject of our earlier paper[24]), the orbital angular momentum of the core state is $l=0$. In this case, nonzero elements of the $3j$ symbols exist only if $l'=l''$, when the squares of the $3j$ symbols take on the values $1/(2l'+1)$. This leads to a simplification of Eq. (15), which becomes

$$\frac{\partial^2\sigma^{20\,1/2}}{\partial E_f\partial\Omega}=\frac{1}{\pi^2}\frac{k_f}{k_i}\kappa\frac{2}{q^4}\sum_{l'}(2l'+1)[F^{l'}_{20,\epsilon l'}(q)]^2\ . \tag{20}$$

Substituting the series expansions (16)–(19) in Eqs. (12) and (20) we can write

$$\frac{\partial^2\sigma^{20\,1/2}}{\partial E_f\partial\Omega}=\frac{1}{\pi^2}\frac{k_f}{k_i}\kappa\frac{2}{q^4}\left\{q^2[\tfrac{1}{3}(I^1_{201})^2]+q^4[\tfrac{1}{36}(I^2_{200})^2+\tfrac{1}{45}(I^2_{202})^2-\tfrac{1}{15}(I^1_{201}I^3_{201})]+O(q^6)\right\}, \tag{21}$$

where

$$I^p_{nll'}=\int_0^\infty\phi_{nl}(r)r^pR_{l'}(\epsilon,r)r^2dr\ . \tag{22}$$

Comparing the terms in (21) proportional to q^2 within the curly brackets with those of the next-highest power of q, namely, q^4, we can deduce that the dipole contributions will dominate only if

$$q^2[\tfrac{1}{3}(I^1_{201})^2]\gg q^4[\tfrac{1}{36}(I^2_{200})^2+\tfrac{1}{45}(I^2_{202})^2-\tfrac{1}{15}(I^1_{201}I^3_{201})]\ . \tag{23}$$

The same condition was deduced in our paper[24] on K-shell excitations by a slightly different argument due to the reversed sign of the term in q^4 in Eq. (42) of that paper. We take the opportunity to correct both the sign and argument here. Since both treatments lead to the same limiting value q_d, all the conclusions of our previous paper remain valid. From the two right-hand subscripts of the integrals $I^p_{nll'}$ in (21) or (23) it is clear that the q^2 term contributes to electronic transitions obeying the dipole selection rule ($\Delta l=\pm1$), while the q^4 term contributes also to monopole ($\Delta l=0$) and quadrupole ($\Delta l=+2$) transitions.

The inequality (23) can be re-expressed as

$$q\ll q_d\ , \tag{24}$$

where

$$q_d=\frac{I^1_{201}}{[\tfrac{1}{12}(I^2_{200})^2+\tfrac{1}{15}(I^2_{202})^2-\tfrac{1}{5}(I^1_{201}I^3_{201})]^{1/2}}\ . \tag{25}$$

B. $L_{\rm II\text{-}III}$ edge

$L_{\rm II}$ and $L_{\rm III}$ edges in XAS or EELS are due to the excitation of core electrons of orbital angular momentum $l=1$; in this case, nonzero elements of the $3j$ symbols exist only if

$l'=0,\ l''=1$,
$l'=1,\ l''=0,2$,
$l'=2,\ l''=1,3$,
$l'=3,\ l''=2,4$,
$\vdots$.

Therefore we may expand (15) as

$$\frac{\partial^2\sigma^{21j}}{\partial E_f\partial\Omega}=\frac{1}{\pi^2}\frac{k_f}{k_i}\kappa\frac{1}{q^4}(2j+1)\{[F^1_{21,\epsilon 0}(q)]^2+[F^0_{21,\epsilon 1}(q)]^2+2[F^2_{21,\epsilon 1}(q)]^2$$
$$+2[F^1_{21,\epsilon 2}(q)]^2+3[F^3_{21,\epsilon 2}(q)]^2+3[F^2_{21,\epsilon 3}(q)]^2+4[F^4_{21,\epsilon 3}(q)]^2+\cdots\} . \quad (26)$$

These expressions differ between the $L_{\rm II}$ and $L_{\rm III}$ edges only due to the appearance of the factor $(2j+1)$ outside the curly brackets, and on the different threshold energies for the excitations of the two core levels. The latter has only a minor effect on the k_f/k_i ratio, while the former gives the statistical 1:2 ratio of the intensities of the $L_{\rm II}$:$L_{\rm III}$ edges. For elements of low atomic number, the spin-orbit energy splitting of the L edges is usually small, and the fine structure on the $L_{\rm III}$ edge runs into the edge discontinuity of the $L_{\rm II}$ edge. The resulting double edge is referred to as the $L_{\rm II\text{-}III}$ edge, and its form may be found by regarding the $L_{\rm III}$ as a doubly-intense $L_{\rm II}$ edge, displaced in energy by the spin-orbit splitting. The superposition of these two absorption-edge structures gives the form of the $L_{\rm II\text{-}III}$ edge. Since both $L_{\rm II}$ and $L_{\rm III}$ edges arise from excitations of core electrons with $l=1$, as we see below, the criteria for the validity of the dipole approximation are not different for the two constituents of the $L_{\rm II\text{-}III}$ edge.

Substituting (16)–(19) in (12) and (26) we find that for core electrons with $l=1$,

$$\frac{\partial^2\sigma^{21j}}{\partial E_f\partial\Omega}=\frac{1}{\pi^2}\frac{k_f}{k_i}\kappa\frac{1}{q^4}(2j+1)\{q^2[\tfrac{1}{9}(I^1_{210})^2+\tfrac{2}{9}(I^1_{212})^2]$$
$$+q^4\left[\tfrac{11}{300}(I^2_{211})^2+\tfrac{1}{75}(I^2_{213})^2-\tfrac{1}{45}(I^1_{210}I^3_{210})-\tfrac{2}{45}(I^1_{212}I^3_{212})\right]+O(q^6)\} . \quad (27)$$

Here too, we see that the terms in q^2 within the curly brackets contain only contributions from dipole ($\Delta l=\pm 1$) transitions, while those in q^4 also contain monopole ($\Delta l=0$) and quadrupole ($\Delta l=\pm 2$) contributions. Here too, the dipole contributions will dominate provided

$$q^2[\tfrac{1}{9}(I^1_{210})^2+\tfrac{2}{9}(I^1_{212})^2]\gg q^4[\tfrac{11}{300}(I^2_{211})^2+\tfrac{1}{75}(I^2_{213})^2-\tfrac{1}{45}(I^1_{210}I^3_{210})-\tfrac{2}{45}(I^1_{212}I^3_{212})] . \quad (28)$$

This can be expressed in the form (24), provided that

$$q_d=\left\{\frac{100[(I^1_{210})^2+2(I^1_{212})^2]}{33(I^2_{211})^2+12(I^2_{213})^2-20(I^1_{210}I^3_{210})-40(I^1_{212}I^3_{212})}\right\}^{1/2} . \quad (29)$$

IV. THE ANALYTIC RADIAL WAVE FUNCTIONS

As in our earlier paper[24] on K-shell excitations, we evaluate the integrals (22) by approximating the radial wave functions on a "hydrogenic" model somewhat similar to that used in the calculation of generalized oscillator strengths.[29,30] On this model, electrons of a particular atomic subshell may be considered to move under the influence of a central Coulombic potential of effective nuclear charge

$$Z^*=Z-s , \quad (30)$$

where s is known as a shielding constant,[31] whose magnitude depends on the electron shell being considered.

Slater[31] has given the following prescriptions for the values of s and Z^*:

(1) Atomic electrons are divided into the following groups of subshells, each having a different shielding constant, namely, 1s; 2s, p; 3s, p; 3d; 4s, p; 4d; 4f; 5s, p; 5d; etc. That is, the s and p subshells of a given shell are grouped together, but the d and f subshells are separated.

(2) The value of the shielding constant s for a particular subshell of a given element is determined by the following contributions: (a) nothing from any shell outside the one considered, (b) an amount 0.35 from each other electron in the group considered (except in the 1s group, where 0.30 is used instead), and (c) if the subshell considered is s or p, an amount 0.85 from each electron with total quantum number less by one, and an amount 1.00 from each electron still further in, but if the shell is a d or f, an amount 1.00 from every electron inside it.

For example, for O, $Z=8$, with two 1s, two 2s, and four 2p electrons, for electrons of the second shell ($n=2$),

$$s=5(0.35)+2(0.85)=3.45$$

and $Z^*=8-3.45=4.55$. For L-shell electrons of all elements with Z greater than or equal to 10(Ne),

$$s=7(0.35)+2(0.85)=4.15 .$$

Slater suggested that, with these values of Z^*, $2s$ and $2p$ wave functions are well approximated by

$$\phi_{20}=NZ^{*3/2}(2-Z^*r)e^{-Z^*r/2} \tag{31}$$

and

$$\phi_{21}=NZ^{*5/2}re^{-Z^*r/2}\,, \tag{32}$$

where N is a normalization constant.

The corresponding radial wave functions $R_l(\epsilon,r)$ of positive energy ϵ are taken to be the Coulomb wave functions:[32]

$$R_l(\epsilon,r)=\frac{1}{(2l+1)!}\exp\left[\frac{\pi Z^*}{2k}\right](2kr)^l\left|\Gamma\left[l+1-\frac{iZ^*}{k}\right]\right|e^{-ikr}{}_1F_1\left[l+1+\frac{iZ^*}{k},2l+2,2ikr\right]\,, \tag{33}$$

expressed in terms of $k(=\sqrt{2\epsilon})$, the wave vector of the ejected atomic electron of energy ϵ. Also in the above expression Γ and ${}_1F_1$ are the gamma and confluent hypergeometric functions, respectively. In the evaluation below of the radial integrals (22), the value of Z^* in (33) is taken to be the same as that of the core state appearing in the integral, since in the region of overlap with that core state, the effective nuclear charge for the excited state is expected to be about the same as that of the core state.

V. EVALUATION OF q_d

A. L_1 edge

Using the integral relation[33]

$$\int_0^\infty e^{-st}t^{b-1}{}_1F_1(a,c,k't)=\Gamma(b)s^{-b}F(a,b,c,k's^{-1}) \tag{34}$$

provided

$$|k's^{-1}|<1\,, \tag{35}$$

where F represents the hypergeometric function,[34] and our analytic radial wave functions (31) and (33), the radial integrals (22) for the excitations of a $2s$ electron ($n=2$, $l=0$) may be written in the closed form:

$$\begin{aligned}I^p_{20l'}=NZ^{*3/2}&\frac{1}{(2l'+1)!}\exp\left[\frac{\pi Z^*}{2k}\right](2k)^{l'}\left|\Gamma\left[l'+1-i\frac{Z^*}{k}\right]\right|\\
&\times\left\{2\Gamma(p+l'+3)\left[\frac{Z^*}{2}+ik\right]^{-(p+l'+3)}F\left[l'+1+i\frac{Z^*}{k},p+l'+3,2l'+2,\frac{4ik}{Z^*+2ik}\right]\right.\\
&\quad -Z^*\Gamma(p+l'+4)\left[\frac{Z^*}{2}+ik\right]^{-(p+l'+4)}\\
&\quad\left.\times F\left[l'+1+i\frac{Z^*}{k},p+l'+4,2l'+2,\frac{4ik}{Z^*+2ik}\right]\right\}\,.\end{aligned} \tag{36}$$

Substituting (36) into (25), we deduce that

$$q_d=2k|1-i\alpha|\frac{A}{\sqrt{B}}\,, \tag{37}$$

where

$$A=F(2+i\alpha,5,4;z)+i5\alpha(2-i\alpha)^{-1}F(2+i\alpha,6,4;z)\,, \tag{38}$$

$$\begin{aligned}B=&3[F(1+i\alpha,5,2;z)]^2-75\frac{\alpha^2}{(2-i\alpha)^2}[F(1+i\alpha,6,2;z)]^2\\
&+\frac{192}{5}\frac{|1-i\alpha|^2|2-i\alpha|^2}{(2-i\alpha)^4}[F(3+i\alpha,7,6;z)]^2-\frac{9408}{5}\frac{a^2|1-i\alpha|^2|2-i\alpha|^2}{(2-i\alpha)^6}[F(3+i\alpha,8,6;z)]^2\\
&+\frac{96|1-i\alpha|^2}{(2-i\alpha)^2}F(2+i\alpha,5,4;z)F(2+i\alpha,7,4;z)-3360\frac{\alpha^2|1-i\alpha|^2}{(2-i\alpha)^4}F(2+i\alpha,6,4;z)F(2+i\alpha,8,4;z)\\
&+i\alpha\left\{\frac{30}{(2-i\alpha)}F(1+i\alpha,5,2;z)F(1+i\alpha,6,2;z)\right.\end{aligned}$$

$$+\frac{2688}{5}\frac{|1-i\alpha|^2|2-i\alpha|^2}{(2-i\alpha)^5}F(3+i\alpha,7,6;z)F(3+i\alpha,8,6;z)$$

$$+94\frac{|1-i\alpha|^2}{(2-i\alpha)^3}[7F(2+i\alpha,5,4;z)F(2+i\alpha,8,4;z)+5F(2+i\alpha,6,4;z)F(2+i\alpha,7,4;z)]\Bigg\}, \tag{39}$$

and

$$\alpha=\frac{Z^*}{k}, \tag{40}$$

$$z=\frac{4}{2-i\alpha}. \tag{41}$$

B. $L_{\text{II-III}}$ edge

Using (32) and (33) in (22) we find that, for $2p$ core electron excitations ($n=2$, $l=1$),

$$I^{p}_{2l'}=NZ^{*5/2}\frac{1}{(2l'+1)!}\exp\left[\frac{\pi Z^*}{2k}\right](2k)^{l'}|\Gamma(l'+1-i\alpha)|$$

$$\times\Gamma(p+l'+4)\left[\frac{Z^*}{2}+ik\right]^{-(p+l'+4)}F(l'+1+i\alpha,p+l'+4,2l'+2;z). \tag{42}$$

Substituting (42) into (29), we deduce in this case,

$$q_d=k\sqrt{A/B}, \tag{43}$$

where

$$A=(\alpha+i2)\left\{[F(1+i\alpha,5,2;z)]^2+32\frac{|2-i\alpha|^2|1-i\alpha|^2}{(\alpha+i2)^4}[F(3+i\alpha,7,6;z)]^2\right\}, \tag{44}$$

$$B=528\frac{|1-i\alpha|^2}{(\alpha+i2)^2}[F(2+i\alpha,7,4;z)]^2+218.45\frac{|3-i\alpha|^2|2-i\alpha|^2|1-i\alpha|^2}{(\alpha+i2)^6}[F(4+i\alpha,9,8;z)]^2$$

$$+24F(1+i\alpha,5,2;z)F(1+i\alpha,7,2;z)+14\,336\frac{|2-i\alpha|^2|1-i\alpha|^2}{(\alpha+i2)^4}F(3+i\alpha,7,6;z)F(3+i\alpha,9,6;z), \tag{45}$$

and

$$\alpha=\frac{Z^*}{k}, \tag{46}$$

$$z=\frac{4}{2-i\alpha}. \tag{47}$$

The hypergeometric functions F, may be evaluated from the power series[34]

$$F(a,b,c;z)=1+\frac{ab}{1!c}z+\frac{a(a+1)b(b+1)}{2!c(c+1)}z^2+\frac{a(a+1)\cdots(a+n-1)b(b+1)\cdots(b+n-1)}{n!c(c+1)\cdots(c+n-1)}z^n+\cdots, \tag{48}$$

which is convergent if $|z|<1$. This is equivalent to the condition (35) and they both require that

$$k<\frac{Z^*}{2\sqrt{3}} \tag{49}$$

for L-shell excitations.

VI. NUMERICAL RESULTS AND DISCUSSION

The preceding analysis shows that, at least within the limit set by Eq. (49), and for core excitation from a given subshell, the upper limit q_d of the magnitude of the momentum transfer vector for dipole excitations is a function of just two variables, namely, the effective nuclear charge Z^* for that subshell, and the wave number k, of the ejected core electrons. In Fig. 1 the variation of q_d with the atomic number Z for $k=1$ is plotted for L_{I}-shell excitations (solid line) and for the $L_{\text{II-III}}$ (dashed line). Bearing in mind the relationship

$$\epsilon=\tfrac{1}{2}k^2 \tag{50}$$

in atomic units, a wave number of $k=1$ a.u. corresponds to an energy of $\frac{1}{2}$ hartree or 13.6 eV, which lies in the

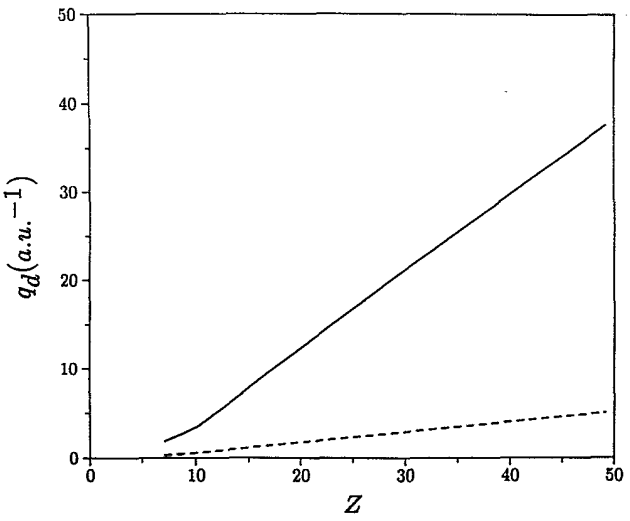

FIG. 1. Plot of q_d vs atomic number Z for $\epsilon=13.6$ eV [$k=1$ (a.u.)$^{-1}$]. Solid line: $L_{\rm I}$ edge EELS; dashed line: $L_{\rm II}$ and $L_{\rm III}$ edge EELS.

ELNES range of energies. Since our theory is nonrelativistic, we have restricted ourselves to a range of chemical elements with atomic number Z up to about 50. Figure 1 shows that for both $L_{\rm I}$ and $L_{\rm II\text{-}III}$ excitations q_d increases nearly linearly with Z, but that in the former case the gradient is rather steeper.

These observations can be understood by noting from Eqs. (12)–(19) that q_d is determined mainly by the radial extent of the core wave function $\phi_{nl}(r)$. This wave function may be thought of as an envelope restricting the range of the integrand on the right-hand side of (12). The integrand becomes negligible for values of r beyond about r_c, the radial extent of the core wave function. Thus the linear terms in q, and hence the dipole terms in (12) will tend to dominate provided that

$$qr_c \ll 1 . \tag{51}$$

Thus, we may estimate that

$$q_d \simeq 1/r_c . \tag{52}$$

The observed increase on Fig. 1 of q_d with Z for both $L_{\rm I}$ and $L_{\rm II\text{-}III}$ edges may therefore be attributed to the well-known fact that the radii of inner electronic shells tend to decrease as Z increases, due to the increase in the nuclear charge and the fact that the outer shells do not contribute significantly to the screening of this charge.

We can also examine the variation of q_d with the energy ϵ of the ejected core electron for particular elements. In order to cover our atomic number range, we study the cases of the elements Si ($Z=14$), Ni ($Z=28$), and Mo ($Z=42$) in Figs. 2–4, respectively. The parts (a) of these figures consider the $L_{\rm I}$ edges, and parts (b) the $L_{\rm II\text{-}III}$ edges. The solid curves of these figures depict the variations of q_d with ϵ. In all cases it is seen that q_d decreases with increasing ϵ, and that the decrease is more marked for the $L_{\rm I}$ than the $L_{\rm II\text{-}III}$ edges. A decrease of q_d with increasing ϵ was also noted in our earlier work on K-edge excitations,[24] and is an effect that could not have been predicted by the simple arguments of the previous paragraph, summarized by Eq. (52), which take into account the nature of only the core wave function. This effect follows from the form of the excited state (33), which we explicitly take account of in our present theory.

As for the restriction implied by Eq. (49), this is equivalent to the condition that

$$\epsilon < \epsilon_{\rm max} , \tag{53}$$

where

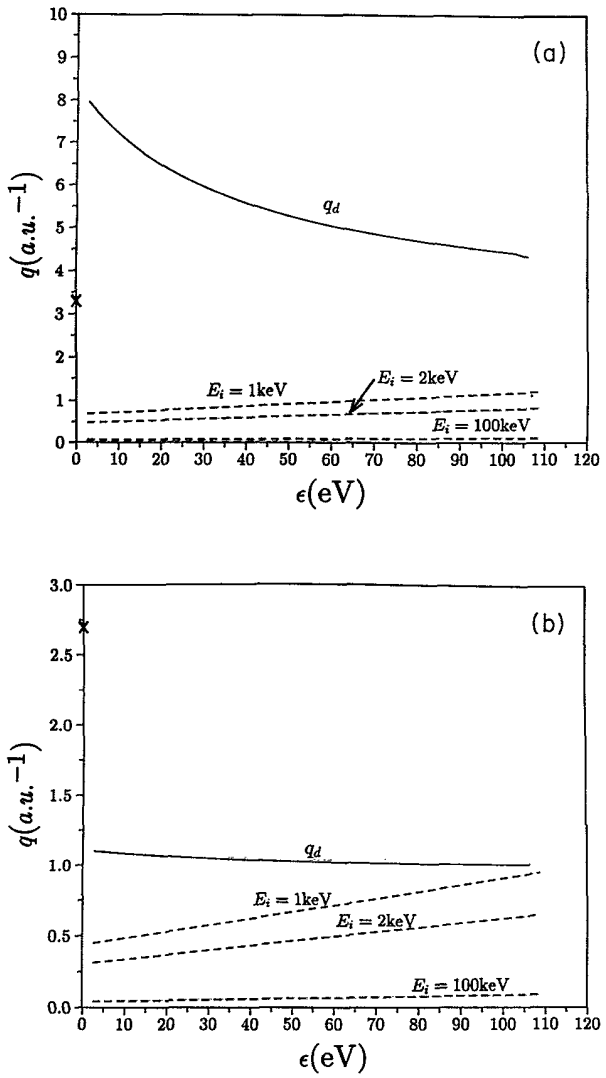

FIG. 2. Comparison of q_d (solid line) and $q_{\rm min}$ (dashed lines) for the Si ($Z=14$) as a function of the energy ϵ of the ejected core electron. The different dashed lines correspond to different energies E_i of the incident primary electrons. (a) The $L_{\rm I}$ edge corresponds to $E_{L_{\rm I}}=150$ eV; (b) the $L_{\rm II\text{-}III}$ edge corresponds to $E_{L_{\rm II\text{-}III}}=99.2$ eV. The crosses on the q_d axis mark the limiting values of $q_{\rm min}$ at the ionization threshold (when $E_i=E_L$).

$$\epsilon_{\max}=\frac{Z^{*2}}{24} . \quad (54)$$

In Table I, we summarize the values of $\epsilon_{\max}$ given by Eq. (54) for a few selected elements. It is clear that our analysis is valid over essentially all of the ELNES range of energies.

In a typical EELS experiment the incident primary electron may suffer much multiple scattering both before and after the inelastic scattering event. As a result, the magnitude and direction of the momentum transfer vector q of our analysis above is generally not simply related to the wave vectors of the incident and detected electrons. In fact, the observed signal may be regarded as an aggregate of inelastic scattering events involving many different inelastic scattering events. Fortunately from the point of view of theoretical analysis, as has been pointed out by several authors (e.g., Refs. 22, 24, and 35), the existence of the squared inverse of q outside the sum over l' in (15) implies that the dominant contributors to the measured EELS signal are those loss events with the smallest q. These correspond to forward inelastic scattering when q takes on the value[36–39]

$$q_{\min}=k_i-k_f . \quad (55)$$

Thus in practice, in a typical EELS experiment on a sample of condensed matter, the dipole approximation would be expected to be satisfied if

TABLE I. Values of $\epsilon_{\max}$ for various elements for L-edge.

Element	Z	hartrees	eV
Al	13	3.26	88.7
Ti	22	13.28	361.2
Cu	29	25.73	699.9
Sr	38	47.74	1298.5
Nb	41	56.58	1539.0
Ag	47	76.51	2081.1

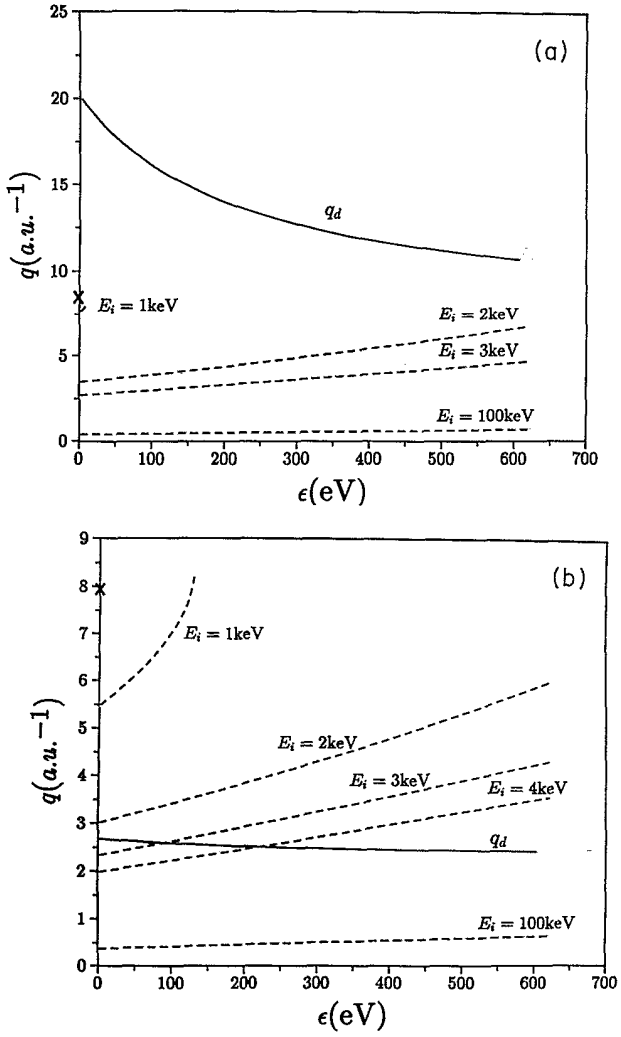

FIG. 3. Same as Fig. 2 but for Ni ($Z=28$). (a) The $L_{\rm I}$ edge corresponds to $E_{L_{\rm I}}=987$ eV; (b) the $L_{\rm II\text{-}III}$ edge corresponds to $E_{L_{\rm II\text{-}III}}=868.5$ eV.

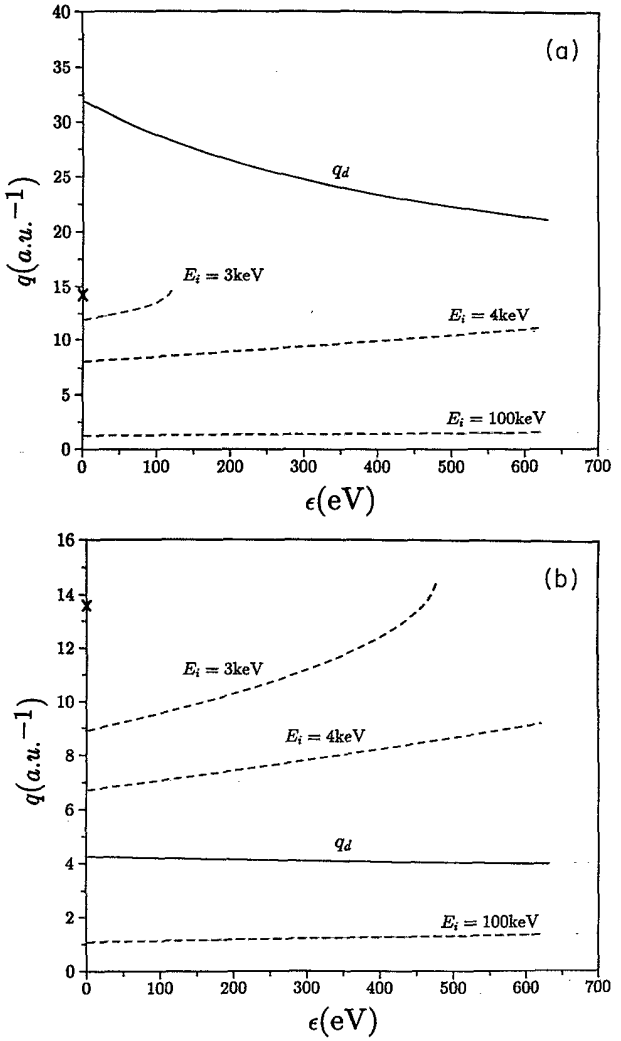

FIG. 4. Same as Fig. 2 but for Mo ($Z=42$). (a) The $L_{\rm I}$ edge corresponds to $E_{L_{\rm I}}=2880$ eV; (b) the $L_{\rm III}$ edge corresponds to $E_{L_{\rm III}}=2520$ eV.

$$q_{\min} \ll q_d \ . \tag{56}$$

From Eq. (55), it follows that

$$q_{\min} = \sqrt{2E_i} - \sqrt{2E_f} \ , \tag{57}$$

where

$$E_f = E_i - \Delta E \tag{58}$$

and

$$\Delta E = E_L + \epsilon \ , \tag{59}$$

where E_L is the ionization energy of the core electron under consideration. Thus we may write

$$q_{\min} = \sqrt{2E_i}[1-(1-\Delta E/E_i)^{1/2}] \ . \tag{60}$$

The requirement that $E_f \geq 0$ implies that ϵ can range from zero up to $E_i - E_L$; the dashed lines in Figs. 2–4 show the variation of $q_{\min}$ against ϵ for several different incident electron energies E_i for the excitation of the L edges of Si, Ni, and Mo. Where possible, the value of ϵ is allowed to vary from zero to about 650 eV to cover the near edge as well as EXELFS ranges.

In reflection EELS experiments, such as those used for surface studies, primary incident electron energies tend to lie in the range of a few hundred to about 3 keV.[40] EELS experiments in electron microscopes, however, use primary energies of the order of 100 keV.[10] In Figs. 2–4, $q_{\min}$ is plotted as a function of the energy ϵ of the ejected electron for several primary electron energies E_i, covering the ranges employed in both reflection and transmission EELS. These curves are compared on the same graphs with the variation of q_d with ϵ. It can be seen that, for all the $L_{\rm I}$ edges, the values of $q_{\min}$ lie well below q_d for all the energies ϵ considered. Therefore it may be concluded that the interpretation of EELS spectra on the dipole approximation for experiments in both the reflection and transmission geometries is well justified for the $L_{\rm I}$ edges of elements in the range studied.

In the case of the $L_{\rm II\text{-}III}$ edge in Si, the above conclusion remains substantially correct, but for the heavier elements Ni and Mo, $q_{\min}$ becomes greater than q_d when E_i is just a few keV, thus raising doubts about the interpretation of such reflection EELS spectra by the x-ray-absorption model. However, note that in all cases, for the $L_{\rm II\text{-}III}$ as well as for the $L_{\rm I}$ edges, $q_{\min}$ lies substantially below q_d for the high primary energies ($\sim$100 keV) employed in transmission EELS. Some experimental support for these results may be found by, for example, comparing the experimental transmission[41] and reflection[9] EELS spectra of the $L_{\rm II\text{-}III}$ edges of Ni and Cu. Substantial differences in the shapes of the spectra are seen. (We are indebted to Dr. Peter Rez for this observation.)

It follows from Eq. (60) that

$$q_{\min} \simeq \frac{\Delta E}{\sqrt{2E_i}} \tag{61}$$

for $\Delta E \ll E_i$. In the near-edge region ΔE is determined primarily by the ionization energy E_L. This is not very different for the $L_{\rm I}$ and $L_{\rm II\text{-}III}$ edges. Hence, $q_{\min}$ is not very different between the parts (a) and (b) of Figs. 2–4. In contrast, q_d is significantly smaller for the $L_{\rm II\text{-}III}$ edge than for the $L_{\rm I}$.

It is the combination of the relative insensitivity of $q_{\min}$ to the angular momentum number of the core state for the same shell, and the strong dependence of q_d to the same quantity which leads, as a consequence of (56), to the markedly different expectations of the validity of the dipole approximation for the $L_{\rm I}$ and $L_{\rm II\text{-}III}$ edges for the heavier elements in reflection EELS.

VII. CONCLUSIONS

We have used a model with analytic representations of both the core and excited electrons to investigate of the validity of the dipole approximation in electron-energy-loss spectroscopy due to L-shell excitations of chemical elements with atomic numbers up to about 50. We derive analytic expressions for the value q_d of the magnitude of the momentum transfer vector q at which nondipole effects become significant. We compare these values with the minimum (and most likely) value of this quantity, namely $q_{\min}$ for the L excitation edges of several representative elements in our atomic number range.

We find that although the dipole approximation is very likely to be good for primary electron energies of the order of 100 keV for all the L edges of all the elements studied, it becomes very questionable for the $L_{\rm II}$ and $L_{\rm III}$ edges of the heavier elements for the low primary energies typically used to enhance surface sensitivity in reflection EELS.

In a future article[42] we plan to extend our analysis to M-shell ($n=3$) excitations.

ACKNOWLEDGMENT

We are grateful to Professor Peter Rez for several stimulating discussions.

[1] P. J. Durham, J. B. Pendry, and C. H. Hodges, Comput. Phys. Commun. **29**, 193 (1982).
[2] E. A. Stern, Phys. Rev. B **10**, 3027 (1974).
[3] P. A. Lee and J. B. Pendry, Phys. Rev. B **11**, 2795 (1975).
[4] C. A. Ashley and S. Doniach, Phys. Rev. B **11**, 1279 (1975).
[5] D. E. Sayers, E. A. Stern, and F. W. Lytle, Phys. Rev. Lett. **27**, 1204 (1977).
[6] J. J. Ritsko, S. E. Schnatterly, and P. C. Gibbons, Phys. Rev. Lett. **32**, 671 (1974).
[7] P. E. Batson and A. J. Craven, Phys. Rev. Lett. **42**, 893 (1979).
[8] M. De Crescenzi, F. Antonangeli, C. Bellini, and R. Rosei, Phys. Rev. Lett. **50**, 1949 (1983).

[9]A. P. Hitchcock and C. H. Teng, Surf. Sci. **149**, 558 (1985).
[10]R. F. Egerton, *Electron-Energy-Loss Spectroscopy in the Electron Microscope* (Plenum, New York, 1986).
[11]J. Tafto and J. Zhu, Ultramicrosc. **9**, 349 (1982).
[12]R. D. Leapman and R. E. Cosslett, J. Phys. D **9**, L29 (1976).
[13]L. A. Grunes and R. D. Leapman, Phys. Rev. B **22**, 3778 (1980).
[14]J. Auerhammer and P. Rez, Phys. Rev. B **40**, 2024 (1989).
[15]P. Aebi, M. Erbudak, F. Vanini, D. D. Vvedensky, and G. Kostorz, Phys. Rev. B **41**, 11 760 (1990).
[16]P. Aebi, M. Erbudak, F. Vanini, D. D. Vvedensky, and G. Kostorz, Phys. Rev. B **42**, 5369 (1990).
[17]C. J. Rossouw and V. M. Maslen, Philos. Mag. A **49**, 743 (1984).
[18]D. K. Saldin and P. Rez, Philos. Mag. B **55**, 481 (1987).
[19]D. K. Saldin, Philos. Mag. B **56**, 515 (1987).
[20]F. Mila and C. Noguera, J. Phys. C **20**, 3863 (1987).
[21]D. K. Saldin, Phys. Rev. Lett. **60**, 1197 (1988).
[22]M. De Crescenzi, L. Lozzi, P. Picozzi, S. Santucci, M. Benfatto, and C. R. Natoli, Phys. Rev. B **39**, 8409 (1989).
[23]P. Rez, Ultramicrosc. **28**, 16 (1989).
[24]D. K. Saldin and J. M. Yao, Phys. Rev. B **41**, 52 (1990).
[25]W. L. Schaich, Phys. Rev. B **29**, 6513 (1984).
[26]A. Messiah, *Quantum Mechanics* (Wiley, New York, 1966), Vol. II.
[27]J. S. Faulkner and G. M. Stocks, Phys. Rev. B **21**, 3222 (1980).
[28]D. D. Vvedensky, D. K. Saldin, and J. B. Pendry, Comput. Phys. Commun. **40**, 421 (1986).
[29]H. A. Bethe, Ann. Phys. **5**, 325 (1930).
[30]R. F. Egerton, Ultramicrosc. **4**, 169 (1979).
[31]J. C. Slater, Phys. Rev. **36**, 57 (1930).
[32]L. D. Landau and E. M. Lifshitz, *Quantum Mechanics* (Pergamon, Oxford, 1977).
[33]I. S. Gradshteyn and I. M. Ryzhik, *Table of Integrals, Series and Products* (Academic, New York, 1965).
[34]*Handbook of Mathematical Functions,* edited by M. Abramowitz and I. A. Stegun (Dover, New York, 1972).
[35]R. D. Leapman, P. Rez, and D. F. Mayers, J. Chem. Phys. **72**, 1232 (1980).
[36]M. Inokuti, Rev. Mod. Phys. **43**, 297 (1971).
[37]C. J. Powell, Surf. Sci. **44**, 29 (1974).
[38]A. G. Nassiopoulos and J. Cazaux, Surf. Sci. **149**, 313 (1985).
[39]A. G. Nassiopoulos and J. Cazaux, Surf. Sci. **165**, 203 (1986).
[40]M. De Crescenzi and G. Chiarello, J. Phys. C **18**, 3595 (1985).
[41]C. C. Ahn and O. L. Krivanek, *EELS Atlas* (Arizona State University, Tempe, 1983).
[42]Y. Ueda and D. K. Saldin (unpublished).